Pluto's ephemeris from ground-based stellar occultations (1988–2016)

J. Desmars, E. Meza, B. Sicardy, M. Assafin, J. I B Camargo, F. Braga-Ribas, G. Benedetti-Rossi, A. Dias-Oliveira, B. Morgado, A. R Gomes-Júnior, et al.

Astronomy & Astrophysics

Pluto's ephemeris from ground-based stellar occultations (1988–2016)

J. Desmars[1], E. Meza[1], B. Sicardy[1], M. Assafin[2], J. I. B. Camargo[3], F. Braga-Ribas[4,3,1], G. Benedetti-Rossi[3], A. Dias-Oliveira[5,3], B. Morgado[3], A. R. Gomes-Júnior[6,2], R. Vieira-Martins[3], R. Behrend[7], J. L. Ortiz[8], R. Duffard[8], N. Morales[8], and P. Santos Sanz[8]

[1] LESIA, Observatoire de Paris, Université PSL, CNRS, Sorbonne Université, Univ. Paris Diderot, Sorbonne Paris Cité, 5 place Jules Janssen, 92195 Meudon, France
e-mail: josselin.desmars@obspm.fr

[2] Observatório do Valongo/UFRJ, Ladeira Pedro Antonio 43, Rio de Janeiro, RJ 20080-090, Brazil

[3] Observatório Nacional/MCTIC, Laboratório Interinstitucional de e-Astronomia-LIneA and INCT do e-Universo, Rua General José Cristino 77, Rio de Janeiro 20921-400, Brazil

[4] Federal University of Technology – Paraná (UTFPR/DAFIS), Rua Sete de Setembro 3165, 80230-901 Curitiba, Brazil

[5] Escola SESC de Ensino Médio, Avenida Ayrton Senna 5677, Rio de Janeiro, RJ 22775-004, Brazil

[6] UNESP – São Paulo State University, Grupo de Dinâmica Orbital e Planetologia, 12516-410 Guaratinguetá, Brazil

[7] Geneva Observatory, 1290 Sauverny, Switzerland

[8] Instituto de Astrofísica de Andalucía (IAA-CSIC), Glorieta de la Astronomía s/n, 18008 Granada, Spain

ABSTRACT

Context. From 1988 to 2016, several stellar occultations have been observed to characterise Pluto's atmosphere and its evolution. From each stellar occultation, an accurate astrometric position of Pluto at the observation epoch is derived. These positions mainly depend on the position of the occulted star and the precision of the timing.

Aims. We present 19 Pluto's astrometric positions derived from occultations from 1988 to 2016. Using *Gaia* DR2 for the positions of the occulted stars, the accuracy of these positions is estimated at $2-10$ mas, depending on the observation circumstances. From these astrometric positions, we derive an updated ephemeris of Pluto's system barycentre using the NIMA code.

Methods. The astrometric positions were derived by fitting the light curves of the occultation by a model of Pluto's atmosphere. The fits provide the observed position of the centre for a reference star position. In most cases other publications provided the circumstances of the occultation such as the coordinates of the stations, timing, and impact parameter, i.e. the closest distance between the station and centre of the shadow. From these parameters, we used a procedure based on the Bessel method to derive an astrometric position.

Results. We derive accurate Pluto's astrometric positions from 1988 to 2016. These positions are used to refine the orbit of Pluto's system barycentre providing an ephemeris, accurate to the milliarcsecond level, over the period $2000-2020$, allowing for better predictions for future stellar occultations.

Key words. astrometry – celestial mechanics – ephemerides – occultations – Kuiper belt objects: individual: Pluto

1. Introduction

Stellar occultation is a unique technique to obtain the physical parameters of distant objects or to probe their atmosphere and surroundings. For instance, Meza et al. (2019) have used 11 stellar occultations by Pluto from 2002 to 2016 to study the evolution of Pluto's atmosphere. Meanwhile, occultations allow an accurate determination of the relative position of the centre of the body compared to the position of the occulted star, leading to an accurate astrometric position of Pluto at the time of occultation if the star position is also known accurately.

The accuracy of the position of the body mainly depends on the knowledge of the shape and size of the body, modelling of the atmosphere, precision of the timing system, velocity of the occultation, exposure time of the camera, precision of the stellar position, and magnitude of the occulted star. Since the publication of the *Gaia* catalogues in September 2016 for the first release (Gaia Collaboration 2016) and moreover with the second release in April 2018 (Gaia Collaboration 2018) including proper

motions and trigonometric parallaxes of the stars, the precision of the stellar catalogues can now reach a tenth of a milliarcsecond. For comparison, before *Gaia* catalogues, the precision of stellar catalogues such as UCAC2 (Zacharias et al. 2004) or UCAC4 (Zacharias et al. 2013), was about $50-100$ mas per star including zonal errors. With *Gaia*, the precision of positions deduced from occultations is expected to be around few milliarcseconds, taking into account the systematic errors. Thanks to the accuracy of the *Gaia* DR2 catalogue, occultations can provide the most accurate astrometric measurement of a body in the outer solar system.

In this paper, we present the astrometric positions we derived from occultations presented in Meza et al. (2019; Sect. 2.1) and in other publications (Sect. 2.2). We detail a method to derive astrometric positions from other publications, knowing the circumstances of occultations: timing and impact parameter (Appendix). Finally, in Sect. 3 we present a refined ephemeris of Pluto's system barycentre and we discuss the improvement in the predictions of future occultations by Pluto at a milliarcsecond level accuracy as well as the geometry of past events (Sect. 4).

2. Astrometric positions from occultations

2.1. Astrometric positions from occultations in Meza et al. (2019)

Meza et al. (2019) provide 11 occultations by Pluto from 2002 to 2016. Beyond the parameters related to Pluto's atmosphere, another product of the occultations is the astrometric position of the body. From the geometry of the event, we determine the position of Pluto's centre of figure (α_c, δ_c). This position corresponds to the observed position of the object at the time of the occultation for a given star position (α_s, δ_s). In particular, the position of the body we derive only depends on the star position. Before *Gaia* catalogues, we determined the star position with our own astrometry. Table 1 gives the position of Pluto's centre and its precision we derived from the geometry of the occultation and the corresponding star position from our astrometry. With *Gaia*, the astrometric position of Pluto's centre can be refined by correcting the star position with the *Gaia* DR2 star position with the relations

$$\alpha = \alpha_c + \alpha_{GDR2} - \alpha_s \qquad (1)$$

$$\delta = \delta_c + \delta_{GDR2} - \delta_s. \qquad (2)$$

This refined position only depends on the *Gaia* DR2 position, which is much more accurate than previous catalogues or our own astrometry. The associated position of the occulted stars in *Gaia* DR2 catalogue $(\alpha_{GDR2}, \delta_{GDR2})$ are listed in Table 2. The positions take into account the proper motions and parallax from *Gaia* DR2. The table also presents the *Gaia* source identifier and the estimated precision of the star position in right ascension and declination at the time of the occultation, taking into account precision of the stellar position and the proper motions as given in *Gaia* DR2, for all the occultations studied in this paper.

Finally, Table 3 provides the absolute position in right ascension and declination of Pluto's centre derived from the geometry and stellar positions of *Gaia* DR2. The residuals related to JPL ephemeris[1] DE436/PLU055 are also indicated as well as the differential positions between Pluto and Pluto's system barycentre used to refine the orbit (see Sect. 3). A flag indicates if the position is used in the NIMAv8 ephemeris determination. Finally, the reconstructed paths of the occultations are presented in Fig. 6.

2.2. Astrometric positions from other publications

Several authors have published circumstances of an occultation by Pluto (e.g. Millis et al. 1993; Sicardy et al. 2003; Elliot et al. 2003; Young et al. 2008; Person et al. 2008; Gulbis et al. 2015; Olkin et al. 2015; Pasachoff et al. 2016, 2017). From these circumstances (coordinates of the observer, mid-time of the occultation, and impact parameter), it is possible to derive an offset between the observation deduced from these circumstances and a reference ephemeris. The procedure, based on the Bessel method used to predict stellar occultations, is described in Appendix A and the details of computation for each occultation are presented in Appendix B. The Pluto's positions deduced from occultations

published in other articles besides those of Meza et al. (2019) are presented in Table 3.

The positions derived from Pasachoff et al. (2016) involving single chord events and faint occulted stars, are not accurate enough to discriminate north and south solutions, i.e. to decide if Pluto's centre as seen from the observing site passed north or south of the star. Finally, these positions were not used in the orbit determination.

3. NIMA ephemeris of Pluto

The NIMA code (Numerical Integration of the Motion of an Asteroid) was developed to refine the orbits of small bodies, in particular trans-Neptunian object (TNOs) and Centaurs studied using the technique of stellar occultations (Desmars et al. 2015). This technique consists of numerical integration of the equations of motion perturbed by gravitational accelerations of the planets (Mercury to Neptune). The Earth and Moon are considered at their barycentre and the masses and the positions of the planets are from JPL DE436.

The use of other masses and positions for planetary ephemeris produces insignificant changes; for example, the difference between the solution using DE436 and that using INPOP17a (Viswanathan et al. 2017) for Pluto, is less than 0.06 mas for the 1985−2025 period. Moreover, there is no need to take into account the gravitational perturbations of the biggest TNOs. For example, by adding the six biggest TNOs (Eris, Haumea, 2007 OR10, Makemake, Quaoar, and Sedna) in the model, the difference between the solutions with and without the biggest TNOs are about 0.04 mas in right ascension and declination for the 1985−2025 period, which is 100 times smaller than the milliarcsecond-level accuracy of the astrometric positions.

The state vector, i.e. the heliocentric vector of position and velocity of the body at a specific epoch, is refined by fitting to astrometric observations with the least-squares method. The main advantage of NIMA is allowing for the use of observations published in the Minor Planet Center[2] together with unpublished observations or astrometric positions of occultations. The quality of the observations is taken into account with a specific weighting scheme, in particular, it takes advantages of the high accuracy of occultations. Finally, after fitting to the observations, NIMA can provide an ephemeris through a bsp file format readable by the SPICE library[3].

As NIMA is representing the motion of the centre of mass of an object, it allows us to compute the position of the Pluto's system barycentre and not the position of Pluto's centre itself. To deal with positions derived from occultations, we need an additional ephemeris representing the position of Pluto relative to its system barycentre. For that purpose, we use the most recent ephemeris PLU055 developed in 2015. The occultation-derived positions are then corrected from the offset between Pluto and the Pluto's system barycentre (see Table 3) to derive the barycentric positions from the occultations, then used in the NIMA fitting procedure.

The precisions of the positions in right ascension and in declination derived from the occultations are provided in Table 1 for occultations presented in Meza et al. (2019) and in Appendix B

---

[1] DE436 is a planetary ephemerides from JPL providing the positions of the barycentre of the planets, including the barycentre of Pluto's system. This is based on DE430 (Folkner et al. 2014). PLU055 is the JPL ephemeris providing the positions of Pluto and its satellites related to the Pluto's system barycentre, developed by R. Jacobson in 2015 and based on an updated ephemeris of Brozović et al. (2015): https://naif.jpl.nasa.gov/pub/naif/generic_kernels/spk/satellites/plu055.cmt

[2] The Minor Planet Center is in charge of providing astrometric measurements, orbital elements of the solar system small bodies: http://minorplanetcenter.net

[3] The SPICE Toolkit is a library developed by NASA dedicated to space navigation and providing in particular a list of routines related to ephemeris: http://naif.jpl.nasa.gov/naif/index.html

Table 1. Date, timing, and position of Pluto's centre deduced from the geometry and precision, coordinates of the occulted star used to derive the astrometric positions of occultations by Pluto studied in Meza et al. (2019).

Reference date	Pluto's centre position				Position of star	
	Right ascension α_c	σ_α (mas)	Declination δ_c	σ_δ (mas)	Right ascension α_s	Declination δ_s
2002-08-21 07:00:32	16h58m49.4393s	0.2	−12°51′31.944″	0.1	16h58m49.4360s	−12°51′31.920″
2007-06-14 01:27:00	17h50m20.7368s	0.1	−16°22′42.210″	0.2	17h50m20.7392s	−16°22′42.210″
2008-06-22 19:07:28	17h58m33.0303s	0.2	−17°02′38.504″	0.2	17h58m33.0138s	−17°02′38.349″
2008-06-24 10:37:00	17h58m22.3959s	0.1	−17°02′49.177″	0.7	17h58m22.3930s	−17°02′49.349″
2010-02-14 04:45:00	18h19m14.3681s	0.2	−18°16′42.125″	0.5	18h19m14.3851s	−18°16′42.313″
2010-06-04 15:34:00	18h18m47.9476s	0.3	−18°12′51.922″	1.3	18h18m47.9349s	−18°12′51.794″
2011-06-04 05:42:00	18h27m53.8235s	0.3	−18°45′30.741″	0.3	18h27m53.8249s	−18°45′30.725″
2012-07-18 04:13:00	18h32m14.6748s	0.1	−19°24′19.307″	0.1	18h32m14.6720s	−19°24′19.295″
2013-05-04 08:22:00	18h47m52.5333s	0.1	−19°41′24.403″	0.1	18h47m52.5322s	−19°41′24.374″
2015-06-29 16:02:00	19h00m49.7122s	0.1	−20°41′40.399″	0.1	19h00m49.4796s	−20°41′40.778″
2016-07-19 20:53:45	19h07m22.1164s	0.1	−21°10′28.242″	0.4	19h07m22.1242s	−21°10′28.445″

Table 2. *Gaia* DR2 source identifier, right ascension and declination and their standard deviation (in milliarcseconds) at epoch and magnitude of the stars of the catalogue *Gaia* DR2 involved in occultations presented in this paper.

Date	*Gaia* source identifier	Right ascension	Declination	σ_α	σ_δ	Gmag
1988-06-09	3652000074629749376	14h52m09.962000s	+00°45′03.30297″	2.14	2.06	12.1
2002-07-20	4333071455580364160	17h00m18.029957s	−12°41′42.01220″	1.12	0.73	12.6
2002-08-21	4333042833914281856	16h58m49.431538s	−12°51′31.85910″	1.87	1.12	15.4
2006-06-12	4124931567980280832	17h41m12.074271s	−15°41′34.47421″	0.63	0.49	14.7
2007-03-18	4149912550502784384	17h55m05.699098s	−16°28′34.36682″	0.74	0.60	14.8
2007-06-14	4147858103406546048	17h50m20.744804s	−16°22′42.22719″	0.83	0.73	15.3
2008-06-22	4144621347334603520	17h58m33.013236s	−17°02′38.39643″	0.67	0.54	12.3
2008-06-24	4144621244254585728	17h58m22.390423s	−17°02′49.36558″	0.93	0.78	15.6
2010-02-14	4096385295578625536	18h19m14.378482s	−18°16′42.35590″	0.50	0.42	10.3
2010-06-04	4096389556186605568	18h18m47.930034s	−18°12′51.82967″	0.37	0.31	14.8
2011-06-04	4093175335706340480	18h27m53.819996s	−18°45′30.78871″	0.62	0.50	16.4
2011-06-23	4093163211131448704	18h25m55.479351s	−18°48′07.09094″	0.35	0.31	14.0
2012-07-18	4092849712861519360	18h32m14.673688s	−19°24′19.34329″	0.19	0.17	14.4
2013-05-04	4086200313156846336	18h47m52.531982s	−19°41′24.39714″	0.10	0.09	14.2
2014-07-23	4085914882468876672	18h49m31.736687s	−20°22′23.82473″	0.21	0.19	17.2
2014-07-24	4085914745029913216	18h49m26.511650s	−20°22′36.98627″	0.39	0.35	18.1
2015-06-29	4084956039611370112	19h00m49.474124s	−20°41′40.81016″	0.04	0.04	12.0
2016-07-19	4082062610353732096	19h07m22.117772s	−21°10′28.43508″	0.05	0.05	13.9

Notes. The coordinates and their precision are provided for the epoch of the occultation taking into account the proper motions and parallax, and their precision.

for other publications. This precision is deduced from a specific model and reduction (for occultations in Meza et al. 2019) and from the precisions of timing and impact parameters (for other publications) without any estimation of systematic errors. For a realistic estimation of the orbit accuracy, the weighting scheme in the orbit fit needs to take into account the systematic errors (see Desmars et al. 2015 for details). The global accuracy for the positions used in the fitting depends on the accuracy of the stellar positions (from 0.1 to 2 mas), the precision of the derived position (from 0.1 mas to 11 mas), and the accuracy of the Pluto body-Pluto system barycentre ephemeris (estimated to 1−5 mas).

The errors on Pluto's centre determination have in fact various sources: the noise present in each occultation light curve and the spatial distribution of the occultation chords across the body. Assuming a normal noise, a formal error on the centre of the

planet can then be derived, using a classical least-squares fitting and χ^2 estimation. However, other systematic errors may also be present, such as problems in the absolute timing registration and slow sky transparency variations that make the photometric noise non-Gaussian. Finally, the particular choice of the atmospheric model may also induce systematic biases in the centre determination. All those systematic errors are difficult to trace back. In that context, it is instructive to compare the reconstructions of the geometry of a given occultation by independent groups that used different chords and different Pluto's atmospheric models. For example, occultations on 21 August 2002, 4 May 2013, and 29 June 2015 (see Table 4) indicate differences of few milliarcseconds, which is much higher than the respective internal precisions (order of 0.1 mas). Case by case studies should be undertaken to explain those inconsistencies. This remains out of the scope of this paper. Meanwhile, for the weighting scheme

Table 3. Right ascension and declination of Pluto deduced from occultations, residuals (O–C) in milliarcseconds related to JPL DE436/PLU055 ephemeris, and differential coordinates (PLU-BAR) between Pluto and Pluto barycentre system position from PLU055 ephemeris.

	Pluto's coordinates		O–C (mas)		PLU-BAR (mas)			
Date (UTC)	Right ascension	Declination	$\Delta\alpha\cos(\delta)$	$\Delta\delta$	$\Delta\alpha\cos(\delta)$	$\Delta\delta$	Flag	References
1988-06-09 10:39:17.0	14h52m09.96347s	+00°45′03.1506″	19.9	−33.5	−8.8	79.6	*	Millis et al. (1993)
2002-07-20 01:43:39.8	17h00m18.03018s	−12°41′41.9934″	7.7	−4.4	−52.9	24.7	*	Sicardy et al. (2003)
2002-08-21 07:00:32.0	16h58m49.43477s	−12°51′31.8833″	20.6	−10.4	−51.2	48.8	*	This paper
2002-08-21 07:00:32.0	16h58m49.43442s	−12°51′31.8820″	15.4	−9.1	−51.2	48.8	*	Elliot et al. (2003)
2006-06-12 16:25:05.7	17h41m12.07511s	−15°41′34.5896″	9.8	−0.4	−47.0	−40.8	*	Young et al. (2008)
2007-03-18 10:59:33.1	17h55m05.69430s	−16°28′34.0886″	10.7	0.8	67.1	−39.4	*	Person et al. (2008)
2007-06-14 01:27:00.0	17h50m20.74243s	−16°22′42.2275″	14.7	−1.8	−5.2	89.8	*	This paper
2008-06-22 19:07:28.0	17h58m33.02976s	−17°02′38.5534″	14.0	0.0	−59.3	−23.3	*	This paper
2008-06-24 10:37:00.0	17h58m22.39339s	−17°02′49.1932″	17.6	8.1	−35.4	89.6	*	This paper
2010-02-14 04:45:00.0	18h19m14.36152s	−18°16′42.1678″	15.2	3.1	−65.4	55.6	*	This paper
2010-06-04 15:34:00.0	18h18m47.94272s	−18°12′51.9579″	14.9	4.8	47.9	49.2	*	This paper
2011-06-04 05:42:00.0	18h27m53.81859s	−18°45′30.8046″	15.6	9.3	71.7	7.1	*	This paper
2011-06-23 11:23:48.2	18h25m55.47963s	−18°48′06.9712″	16.1	5.5	73.2	0.2	*	Gulbis et al. (2015)
2012-07-18 04:13:00.0	18h32m14.67647s	−19°24′19.3554″	16.9	7.7	55.2	−76.0	*	This paper
2013-05-04 08:21:41.8	18h47m52.53356s	−19°41′24.4265″	18.7	8.4	−74.6	47.9	*	Olkin et al. (2015)
2013-05-04 08:22:00.0	18h47m52.53305s	−19°41′24.4265″	19.3	9.2	−74.6	48.0	*	This paper
2014-07-23 14:25:59.1	18h49m31.74100s	−20°22′23.9915″	30.4	3.7	−7.5	−79.7		Pasachoff et al. (2016)
2014-07-23 14:25:59.1	18h49m31.74048s	−20°22′23.9502″	23.0	44.9	−7.5	−79.7		Pasachoff et al. (2016)
2014-07-24 11:42:20.0	18h49m26.51393s	−20°22′37.1172″	11.3	−14.6	−65.8	−28.7		Pasachoff et al. (2016)
2014-07-24 11:42:20.0	18h49m26.51337s	−20°22′37.0734″	3.4	29.1	−65.8	−28.7		Pasachoff et al. (2016)
2015-06-29 16:02:00.0	19h00m49.70680s	−20°41′40.4308″	22.8	10.7	−41.9	80.3	*	This paper
2015-06-29 16:54:41.4	19h00m49.47778s	−20°41′40.9707″	22.1	12.7	−39.4	81.2	*	Pasachoff et al. (2017)
2016-07-19 20:53:45.0	19h07m22.10999s	−21°10′28.2320″	24.1	11.6	56.5	−71.7	*	This paper

Notes. A flag * is indicated if the position was used in the NIMAv8 ephemeris (see Sect. 3).

in the orbit fit, we adopt the estimated precision presented in Table 4 taking into account an estimation of systematic errors for each occultation.

Figure 1 shows the difference between NIMA[4] and JPLDE436 ephemeris of Pluto's barycentre in right ascension (weighted by $\cos\delta$) and declination. The blue bullets and error bars represent the positions and their estimated precision from our occultations. The red bullets represent the positions from occultations not listed in Meza et al. (2019) as follows: Millis et al. (1993), Sicardy et al. (2003), Elliot et al. (2003), Young et al. (2008), Person et al. (2008), Gulbis et al. (2015), Olkin et al. (2015), and Pasachoff et al. (2017). The grey area represents the one sigma uncertainty of the NIMAv8 ephemeris.

Table 4 and Fig. 2 provide the residuals (O–C) of the positions derived from the occultations, compared with the NIMAv8 ephemeris, and the estimated precision of the positions used in the weighting scheme. After 2011, residuals are mostly below the milliarcsecond level, which is much better than any ground-based astrometric observation of Pluto. In that context, other classical observations of Pluto, such as CCD, appear to be less useful for ephemerides of Pluto during the period covered by the occultations 1988−2016.

Figure 3 shows the difference in right ascension and declination between the most recent ephemerides of Pluto system barycentre: JPL DE436, INPOP17a (Viswanathan et al. 2017) and EPM2017 (Pitjeva & Pitjev 2014) compared to NIMAv8. These differences are mostly due to data and weights used for the orbit determination. They reveal periodic terms in the orbit of Pluto system barycentre that are estimated differently

Table 4. Residuals (O–C) related to NIMAv8 ephemeris of Pluto system barycentre.

Date (UTC)	$\Delta\alpha\cos(\delta)$ (mas)	$\Delta\delta$ (mas)	σ_α (mas)	σ_δ (mas)
1988-06-09	−0.7	1.3	10.0	10.0
2002-07-20	−5.3	3.8	10.0	15.0
2002-08-21 [1]	2.9	−1.1	10.0	10.0
2002-08-21	8.1	−2.4	10.0	10.0
2006-06-12	−4.0	1.2	10.0	10.0
2007-03-18	−4.1	0.6	10.0	10.0
2007-06-14	0.6	−2.2	5.0	5.0
2008-06-22	−0.4	−2.1	5.0	5.0
2008-06-24	2.6	2.2	5.0	5.0
2010-02-14	−1.1	−1.2	5.0	5.0
2010-06-04	−1.3	0.2	5.0	5.0
2011-06-04	−1.7	3.2	5.0	5.0
2011-06-23	−0.2	−0.5	10.0	10.0
2012-07-18	0.2	0.3	5.0	5.0
2013-05-04 [2]	−1.1	−0.2	10.0	10.0
2013-05-04	−0.5	0.6	5.0	5.0
2015-06-29	0.5	−0.1	2.0	2.0
2015-06-29 [3]	−0.7	1.8	10.0	10.0
2016-07-19	−0.1	−0.2	2.0	2.0

Notes. Estimated precision in mas in right ascension and declination used for the fit is also indicated. [1]Taken from Elliot et al. (2003). [2]Taken from Olkin et al. (2015). [3]Taken from Pasachoff et al. (2017).

in orbit determination. As described in Desmars et al. (2015), the one-year period corresponds to the parallax induced by

---

[4] The NIMAv8 ephemeris is available on http://lesia.obspm.fr/lucky-star/nima.php
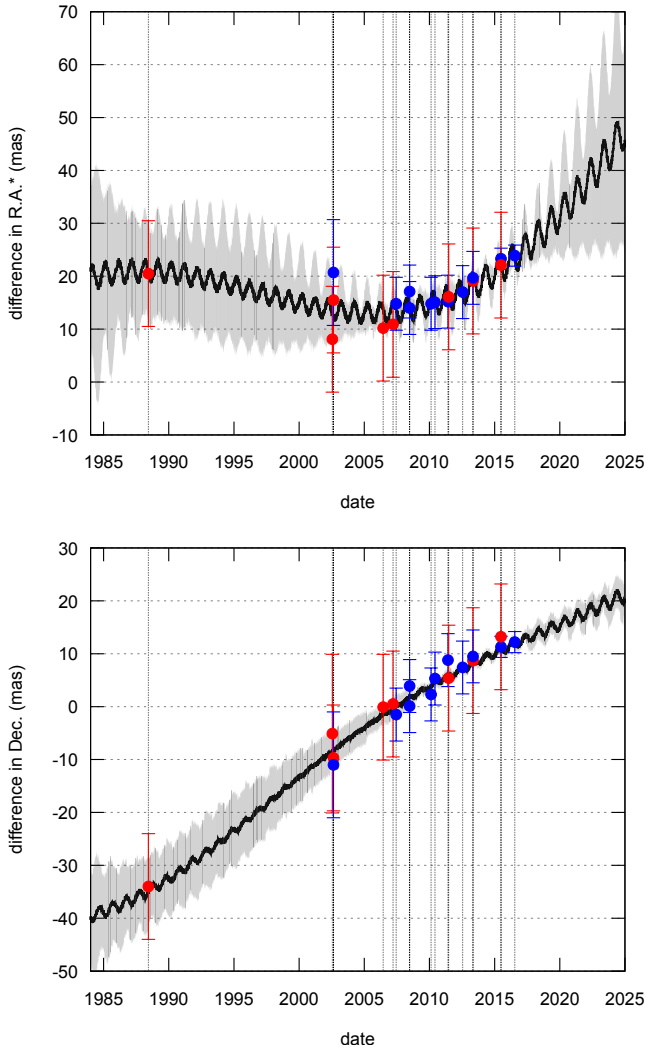
Fig. 1. Difference between NIMAv8 and JPL DE436 ephemeris of Pluto's system barycentre (black line) in right ascension (weighted by $\cos \delta$) and in declination. Blue bullets and their estimated precision in error bar represent the positions coming from the occultations studied in this work and red bullets represent the positions deduced from other publications. The grey area represents the 1σ uncertainty of the NIMA orbit. Vertical grey lines indicate the date of the position for a better reading on the x-axis. The angular diameter of Pluto, as seen from Earth, is about 115 mas, while the atmosphere detectable using ground-based stellar occultations subtends about 150 mas on the sky.

different geocentric distances given by the ephemerides. It is also another good indication of the improvement of the NIMAv8 ephemeris since the differences between these ephemerides reach $50-100$ mas, whereas the estimated precision of NIMAv8 is $2-20$ mas for the same period.

4. Discussion

The NIMA ephemeris allows very accurate predictions of stellar occultation by Pluto in the forthcoming years within a few millisecond levels. In particular, we predicted an occultation of a magnitude 13 star[5] by Pluto on August 15, 2018, above North America to the precision of 2.5 mas, representing only 60 km on the shadow path and a precision of 4 s in time. As shown

---

5 The star position in *Gaia* DR2 at the epoch of the occultation is 19h22m10.4687s in right ascension and −21°58′49.020″ in declination.
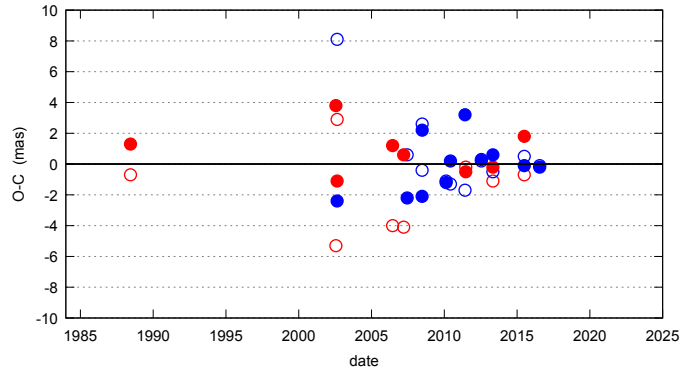
Fig. 2. Residuals of Pluto's system barycentre positions compared to NIMAv8. Circles indicate right ascension weighted by $\cos \delta$ and bullets indicate declination. Blue represents the positions coming from the occultations studied in this work and red represents the positions deduced from other publications.
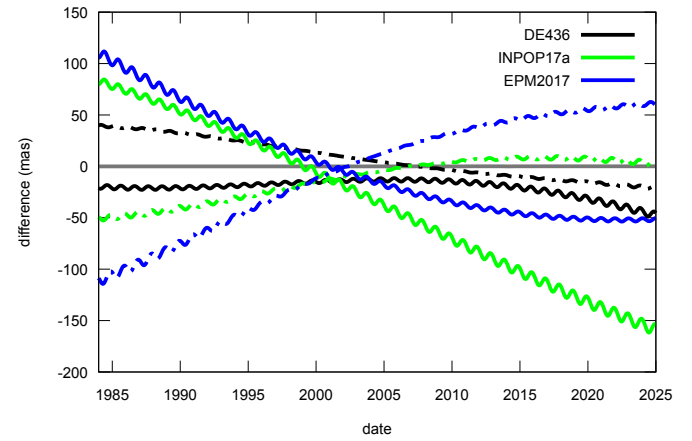

Fig. 3. Difference in right ascension weighted by $\cos \delta$ (solid line) and declination (dotted line) between several ephemerides of Pluto system barycentre: JPL DE436, INPOP17, and EPM2017, compared to NIMAv8.

in Meza et al. (2019), the observation of a central flash allows us to probe the deepest layers of Pluto's atmosphere. The central flash can be observed in an small band about 50 km around the centrality path. By reaching a precision of tens of km, we were able to gather observing stations along the centrality and to highly increase the probability of observing a central flash.

The prediction of the August 15, 2018 Pluto occultation was used to assess the accuracy of our predictions using the NIMA approach. Figure 4 represents the prediction of the occultation by Pluto on August 15, 2018 using two different ephemerides: JPL DE436/PLU055 and NIMAv8/PLU055. The prediction using JPL ephemerides is shifted by 36.8 s and 8 mas south (representing about 190 km) compared to the prediction with NIMAv8 ephemeris. Several stations detected the occultation, some of which reveal a central flash. For instance, observers at George Observatory (Texas, USA) reported a central flash of typical amplitude 20%, compared to the unocculted stellar flux (Blank & Maley, priv. comm.).

As the amplitude of the flash roughly scales as the inverse of the closest approach (C/A) distance of the station to the shadow centre, the amplitude may serve to estimate the C/A distance. A central flash reported by Sicardy et al. (2016) was observed at a station in New Zealand during the June 29, 2015 occultation. It had an amplitude of 13% and a C/A distance of 42 km. Thus, the
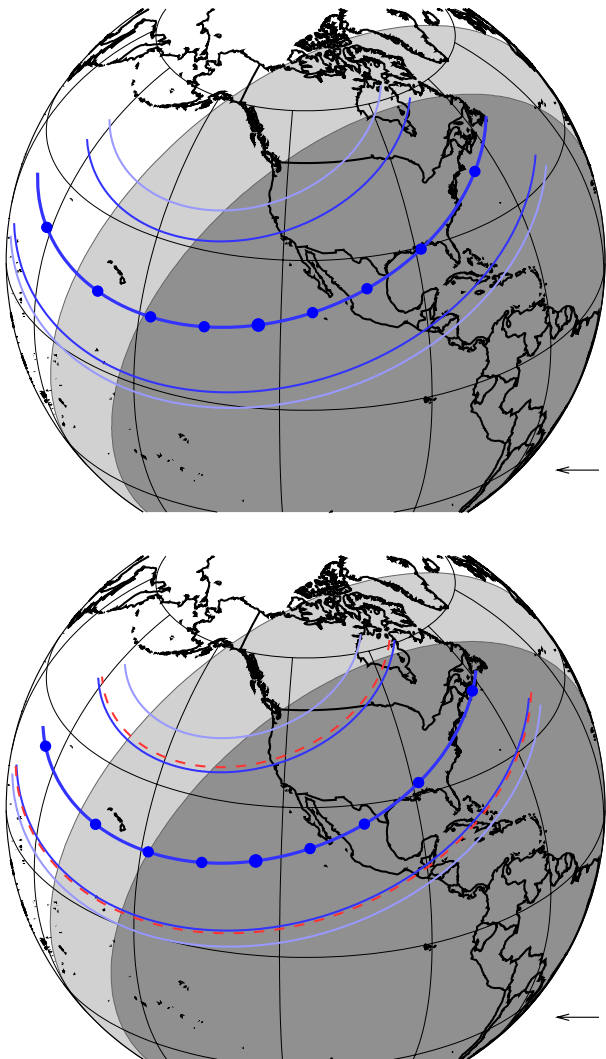
Fig. 4. Prediction of the occultation by Pluto on 15 August 2018, using JPL DE436/PLU055 (*top*) and NIMAv8/PLU055 (*bottom*) ephemerides. The red dashed lines represent the 1σ uncertainty on the path, taking into account the uncertainties of NIMAv8 ephemeris and of the star position. The bullets on the shadow central line are plotted every minute. The dark and light blue thinner lines are the shadow limits corresponding the stellar half-light level and 1% stellar drop level (the practical detection limit), respectively.

flash observed at George Observatory provides an estimated C/A distance of 25 km for that station. This agrees with the value predicted by the NIMAv8/PLU055 ephemeris, to within 3 km, corresponding to 0.12 mas. This is fully consistent with, but smaller than our 2.5 mas error bar quoted above, possibly indicating an overestimation of our prediction errors.

The precision of our predictions remains at few milliseconds up to 2025 (in particular in declination) and it is even more important since the apparent position of Pluto as seen from Earth is moving away from the Galactic centre, making occultations by Pluto more rare.

Another point of interest is to look at past occultations. In particular, for the occultation of August 19, 1985, Brosch & Mendelson (1985) reported a single chord occultation of a magnitude 11.1 star[6] by Pluto, showing a gradual shape

---

[6] The star position in *Gaia* DR2 at the epoch of the occultation is 14h23m43.4575s in right ascension and +03°06′46.874″ in declination.
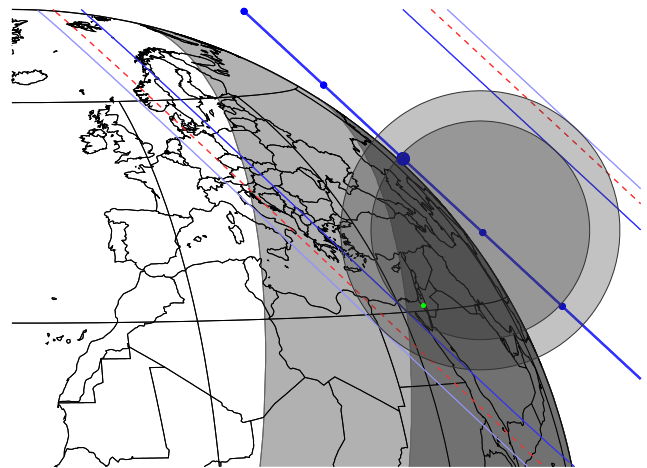
Fig. 5. Postdiction of the Pluto's occultation of 19 August 1985, using NIMAv8/PLU055 ephemerides. The shadow of Pluto at 17:59:54 (the mid-time of the occultation provided in Brosch 1995) is represented. The green bullet represents the WISE observatory. The red dashed lines represent the 1σ uncertainty on the path. Areas in dark grey correspond to full night (Sun elevation below $-18°$) and areas in light grey correspond to twilight (Sun elevation between $-18°$ and $0°$), while daytime regions are in white. The dark and light blue thinner lines are the shadow limits corresponding the stellar half-light level and 1% stellar drop level (the practical detection limit), respectively.

possibly due to Pluto's atmosphere. The observation was performed at Wise observatory in Israel under poor conditions (low elevation, flares from passing planes, close to twilight). Thanks to *Gaia* DR2 providing the proper motion of the star and to NIMAv8, we make a postdiction of the occultation of August 19, 1985 (Fig. 5). The nominal time for the occultation, i.e. the time of the closest approach between the geocentre and centre of the shadow, is 17:58:57.1 (UTC), leading to a predicted mid-time of 17:59:49.8 (UTC) at Wise observatory. Brosch (1995) gave an approximate observed mid-time of the occultation for Wise observatory at 17:59:54 (about 4 s later than the prediction). The predicted shadow of Pluto at the same time is presented in the figure and the location of the observatory is represented as a green bullet. Taking into account the uncertainties of the NIMAv8 ephemeris and of the star position, the uncertainty in time for this occultation is about 20 s, whereas the crosstrack uncertainty on the path is about 10 mas (representing 220 km). This is fully consistent with the fact that the occultation was indeed observed at Wise observatory.

5. Conclusions

Stellar occultations by Pluto provide accurate astrometric positions thanks to *Gaia* catalogues, in particular *Gaia* DR2. We determine 18 astrometric positions of Pluto from 1988 to 2016 with an estimated precision of 2−10 mas.

These positions are used to compute an ephemeris of the barycentre of Pluto system thanks to the NIMA procedure with an unprecedented precision on the 1985−2015 period. This ephemeris NIMAv8 was also used to study the possible occultation of Pluto observed in 1985 to predict the recent occultation by Pluto on August 15, 2018 or the forthcoming occultations[7] with a precision of 2 mas, a result that is impossible to reach with classical astrometry and previous stellar catalogues. In fact, the

---

[7] See the predictions on the Lucky Star webpage http://lesia.obspm.fr/lucky-star/predictions.php
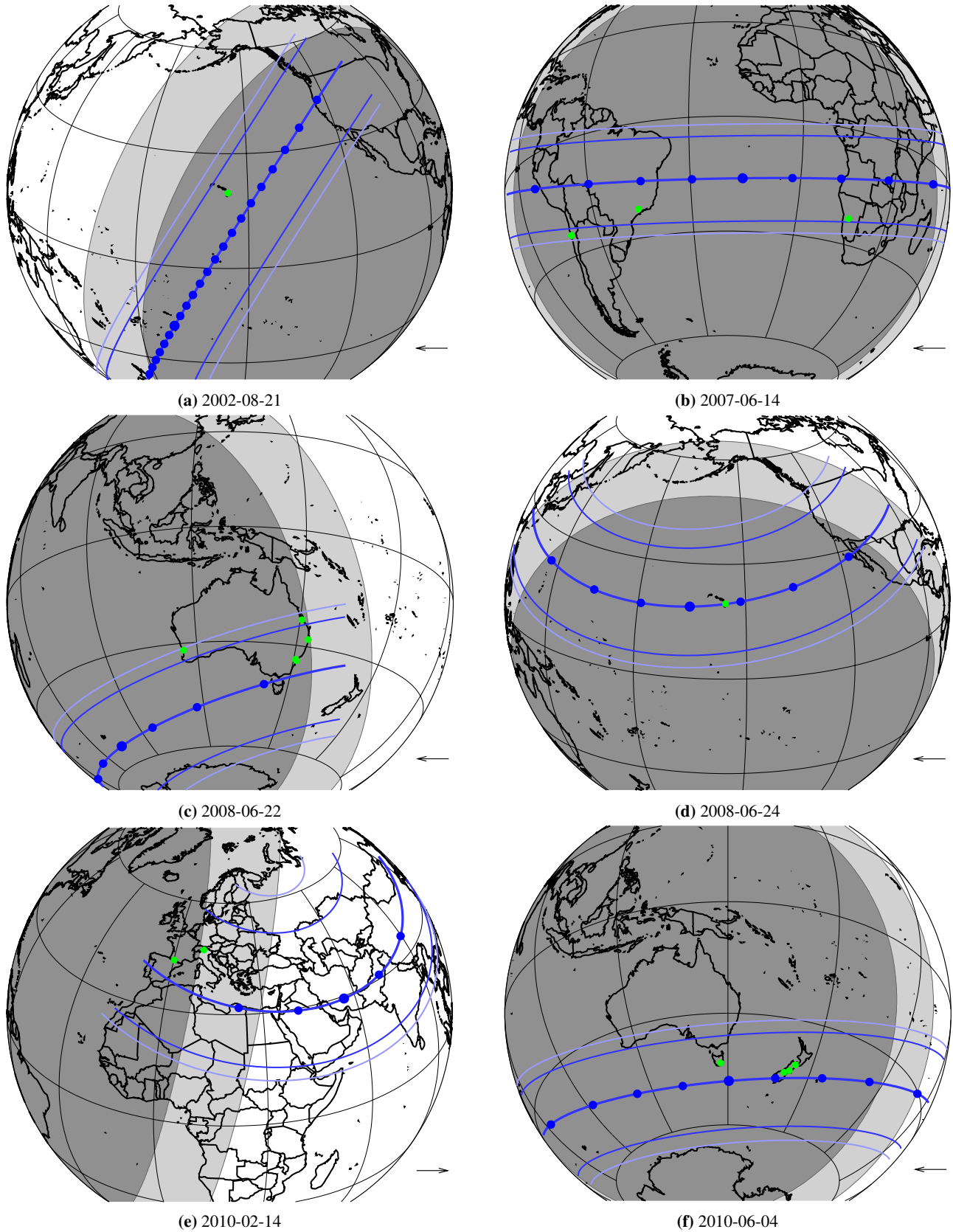
Fig. 6. Reconstruction of Pluto's shadow trajectories on Earth for occultations observed from 2002 to 2016; see details in Meza et al. (2019). The bullets on the shadow central line are plotted every minute, and the black arrow represents the shadow motion direction (see arrow at lower right corner). The dark and light blue thinner lines are the shadow limits corresponding the stellar half-light level and 1% stellar drop level (the practical detection limit), respectively. The green bullets correspond to the sites with positive detection used in the fit. Areas in dark grey correspond to full night (Sun elevation below −18°) and areas in light grey correspond to astronomical twilight (Sun elevation between −18° and 0°), while daytime regions are in white.

(g) 2011-06-04

(h) 2012-07-18

(i) 2013-05-04

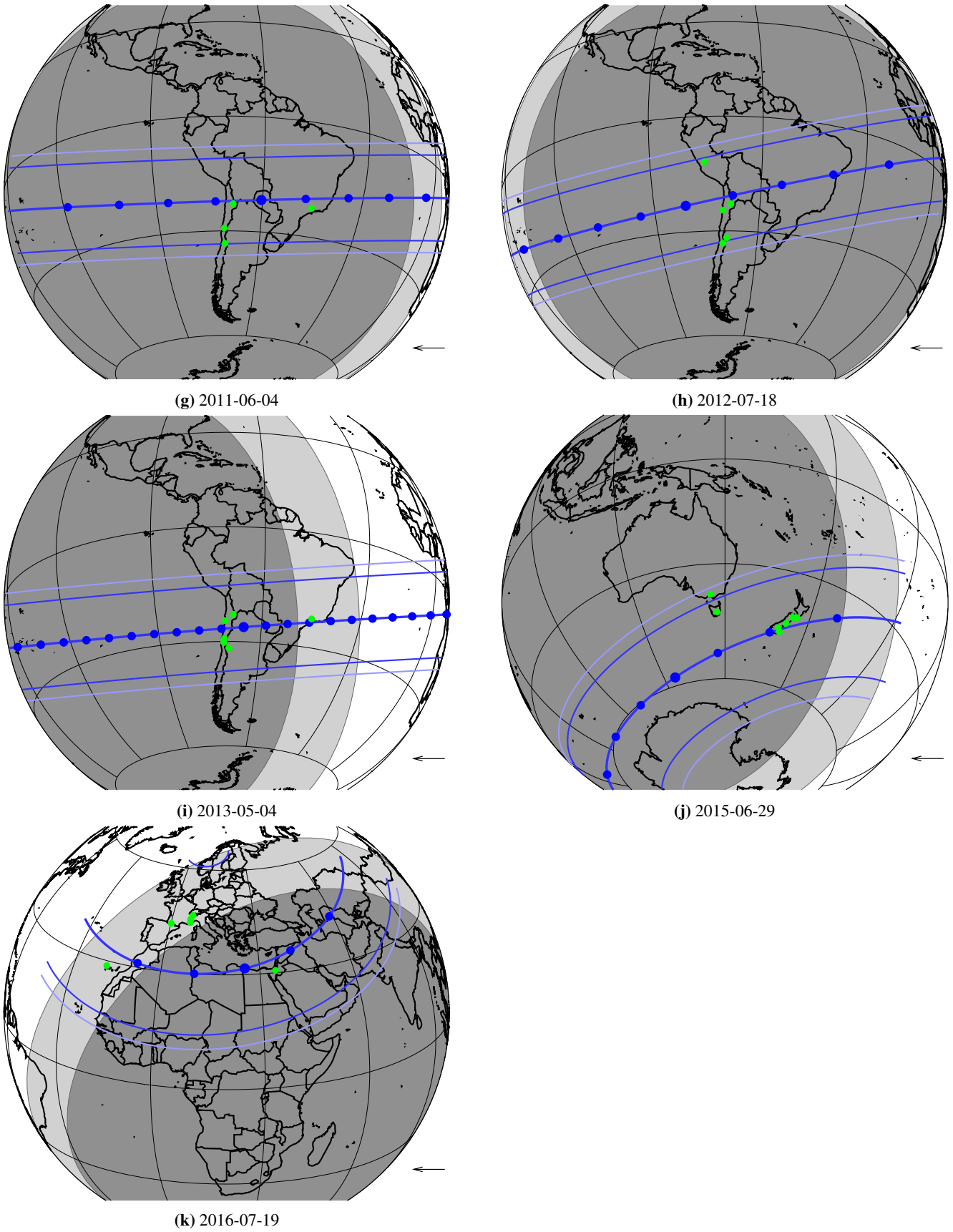(j) 2015-06-29

(k) 2016-07-19

Fig. 6. continued.

presence of the usually unresolved Charon in classical images causes significant displacements of the photocentre of the system with respect to its barycentre. As a consequence, and even modelling the effect of Charon, as in Benedetti-Rossi et al. (2014), accuracies below the 50 mas level are difficult to reach.

This method can be extended, for instance for Chariklo, with an even better accuracy of the order of 1 mas (Desmars et al. 2017) and illustrates the power of stellar occultations not only for better studying those bodies, but also for improving their orbital elements.

References

Benedetti-Rossi, G., Vieira Martins, R., Camargo, J. I. B., Assafin, M., & Braga-Ribas, F. 2014, A&A, 570, A86
Brosch, N. 1995, MNRAS, 276, 571
Brosch, N., & Mendelson, H. 1985, IAU Circ., 4097
Brozović, M., Showalter, M. R., Jacobson, R. A., & Buie, M. W. 2015, Icarus, 246, 317
Desmars, J., Camargo, J. I. B., Braga-Ribas, F., et al. 2015, A&A, 584, A96
Desmars, J., Camargo, J., Bérard, D., et al. 2017, AAS/Division for Planetary Sciences Meeting Abstracts, 49, 216.03
Elliot, J. L., Ates, A., Babcock, B. A., et al. 2003, Nature, 424, 165
Folkner, W., Williams, J., Boggs, D., Park, R., & Kuchynka, P. 2014, JPL IPN Progress Reports 42-196, http://ipnpr.jpl.nasa.gov/progress_report/42-196/196C.pdf
Gaia Collaboration (Brown, A. G. A., et al.) 2016, A&A, 595, A2
Gaia Collaboration (Brown, A. G. A., et al.) 2018, A&A, 616, A1
Gulbis, A. A. S., Emery, J. P., Person, M. J., et al. 2015, Icarus, 246, 226
Meza, E., Sicardy, B., Assafin, M., et al. 2019, A&A, 625, A42
Millis, R. L., Wasserman, L. H., Franz, O. G., et al. 1993, Icarus, 105, 282
Olkin, C. B., Young, L. A., Borncamp, D., et al. 2015, Icarus, 246, 220
Pasachoff, J. M., Person, M. J., Bosh, A. S., et al. 2016, AJ, 151, 97
Pasachoff, J. M., Babcock, B. A., Durst, R. F., et al. 2017, Icarus, 296, 305
Person, M. J., Elliot, J. L., Gulbis, A. A. S., et al. 2008, AJ, 136, 1510
Pitjeva, E. V., & Pitjev, N. P. 2014, Celestial Mech. Dyn. Astron., 119, 237
Sicardy, B., Widemann, T., Lellouch, E., et al. 2003, Nature, 424, 168
Sicardy, B., Talbot, J., Meza, E., et al. 2016, ApJ, 819, L38
Urban, S. E., & Seidelmann, P. K. 2013, Explanatory Supplement to the Astronomical Almanac (University Science Books)
Viswanathan, V., Fianga, A., Gastineau, M., & Laskar, J. 2017, Notes Scientifiques et Techniques de l'Institut de Mécanique Céleste S108, https://www.imcce.fr/inpop/
Young, E. F., French, R. G., Young, L. A., et al. 2008, AJ, 136, 1757
Zacharias, N., Urban, S. E., Zacharias, M. I., et al. 2004, AJ, 127, 3043
Zacharias, N., Finch, C. T., Girard, T. M., et al. 2013, AJ, 145, 44

Appendix A: Method to derive astrometric positions from occultation's circumstances

We present in this section a method to derive an astrometric position from an occultation's observation, knowing the occultation's circumstances. The determination of an occultation's circumstances consists in computing the Besselian elements. The Bessel method makes use of the fundamental plane that passes through the centre of the Earth and perpendicular to the line joining the star and the centre of the object (i.e. the axis of the shadow). The method is for example described in Urban & Seidelmann (2013). The Besselian elements are usually given for the time of conjunction of the star and the object in right ascension but in this paper the reference time is the time of closest angular approach between the star and the object.

The Besselian elements are T_0 the UTC time of the closest approach, H the Greenwich Hour Angle of the star at T_0, x_0 and y_0 the coordinates of the shadow axis at T_0 in the fundamental plane, x' and y' the rates of changes in x and y at T_0, and α_s, δ_s the right ascension and the declination of the star. Their computation are fully described in Urban & Seidelmann (2013).

The quantities x_0, y_0, x', and y' depend on the ephemeris of the body and allow us to represent the linear motion of the shadow at the time of the occultation. In this paper, x_0, y_0 are expressed in Earth radius unit and x', y' are in Earth radius per day.

From T_0, α_s, δ_s, and H, the coordinates[8] of the shadow centre (λ_c, ϕ_c) at T_0 can be derived.

For an observing site, the method requires the local circumstances which are the mid-time of the occultation and the impact parameter ρ, the distance of closest approach between the site, and the centre of the shadow in the fundamental plane. Usually, the impact parameter is given in kilometres and when the occultation has only one chord, two solutions (North and South) can be associated.

The first step is to add a shift to x_0 and y_0 to take into account the impact parameter, i.e. the fact that the observing site is not right on the centrality of the occultation, as follows:

$$x_0 \rightarrow x_0 \pm s \frac{x_0}{\sqrt{x_0^2 + y_0^2}} \tag{A.1}$$

$$y_0 \rightarrow y_0 \pm s \frac{y_0}{\sqrt{x_0^2 + y_0^2}}, \tag{A.2}$$

where s is the ratio of ρ to Earth radius.

Given the longitude λ and the latitude[8] ϕ of the observing site, the coordinates in the fundamental plane are given by

$$u = \cos\phi \sin(\lambda - \lambda_c) \tag{A.3}$$

$$v = \sin\phi \cos\phi_c - \cos\phi \sin\phi_c \cos(\lambda - \lambda_c) \tag{A.4}$$

$$w = \sin\phi \sin\phi_c + \cos\phi \cos\phi_c \cos(\lambda - \lambda_c). \tag{A.5}$$

The time of the closest approach for the observer is given by the relation

$$t_m = T_0 + \frac{(u - x_0)x' + (v - y_0)y'}{x'^2 + y'^2}. \tag{A.6}$$

In fact, t_m, u, v, w are calculated iteratively by replacing λ_c by $\lambda_c - \Omega(t_m - T_0)$, where Ω is the rate of Earth's rotation, to take into account the Earth's rotation during $t_m - T_0$.

---

[8] Latitude refers to geocentric latitude. Usually coordinates provide geodetic latitude that need to be converted to geocentric latitude.

If Δt is the difference between the observed time of the occultation for the observer and the nominal time of the occultation T_0, the correction to apply to the Besselian elements x_0, y_0 are

$$\Delta x = (u - x_0) - x'\Delta t \tag{A.7}$$

$$\Delta y = (v - y_0) - y'\Delta t. \tag{A.8}$$

The quantities $\Delta x, \Delta y$ are determined iteratively and finally transformed into an offset in right ascension and in declination between the observed occultation and the predicted occultation (from the ephemeris).

For single chord occultation, there are two solutions (north and south), meaning that we do not know whether Pluto's centre went north or south of the star as seen from the observing site. Conversely, for multi-chord occultation there is a unique solution. In that case, the astrometric position deduced from the occultation is the reference ephemeris plus the average offset deduced from all the observing sites.

This is a powerful method to derive astrometric positions from occultations. It only requires local circumstances of the occultation for the observing sites such as the mid-time of the occultation and the impact parameter. If the impact parameter is not provided, we can deduce it from the timing of immersion and emmersion knowing the size of the object and assuming it is spherical. Thus, the method can be used for any object.

Appendix B: Astrometric positions from other occultations

In this section, we derive astrometric positions from occultations published in various articles using the method previously presented. The Besselian elements corresponding to the occultations are presented in Table B.7 and the reconstructed shadow trajectories of occultation are presented in Fig. B.1.

B.1. Occultation of June 9, 1988

Millis et al. (1993) presented the June 9, 1988 Pluto occultation. They derived an astrometric solution by giving the impact parameter for the eight stations that recorded the event.

According to the mid-time of the occultation derived from the paper, we determine the following offsets:

For Black Birch, there is only the immersion timing so the mid-time of the occultation cannot be derived. The average offset of this occultation was determined using the same set of the preferred astrometric solution of Millis et al. (1993), i.e. data from Charters Towers, Hobart, Kuiper Airbone Observatory (KAO), and Mont John (see Table B.1).

Finally, we derive the average offset of $\Delta\alpha \cos\delta = +19.9 \pm 0.5$ mas and $\Delta\delta = -33.5 \pm 0.3$ mas.

B.2. Occultation of July 20, 2002

Sicardy et al. (2003) obtained a light curve of the occultation by Pluto near Arica, north of Chile. They derived an astrometric solution of the occultation by giving distance of closest approach to the centre of Pluto's shadow for Arica (975 ± 250 km).

In Arica, the mid-time of the occultation occurs at 01:44:03 (UTC), giving $\Delta t = 23.2$ s. There are two possible solutions but the occultation was also observed at Mamiña[9] in Chile (Buie, priv. comm.) so the only possible solution is that of the south. Finally, we derive the offset of $\Delta\alpha \cos\delta = +7.7 \pm 1.9$ mas and $\Delta\delta = -4.4 \pm 11.2$ mas, assuming a precision of 2 s for the mid-time.

---

[9] The Mamiña coordinates are 20°04′51.00″S and 69°12′00.00″W.

(a) 1988-06-09

(b) 2002-07-20

(c) 2006-06-12

(d) 2007-03-18

(e) 2011-06-23

(f) 2013-05-04
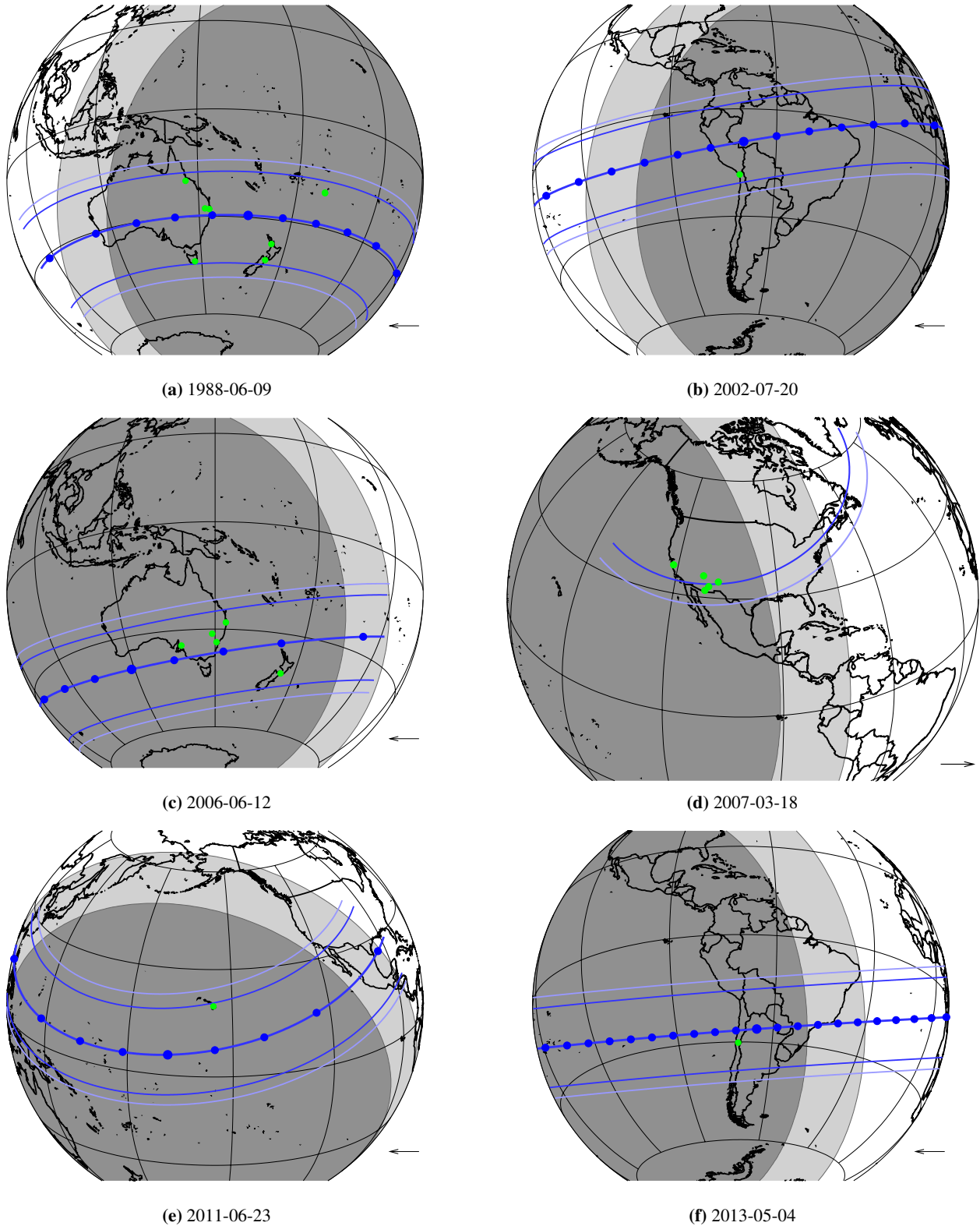
Fig. B.1. Reconstruction of Pluto's shadow trajectories on Earth for occultations presented in other publications from 1988 to 2015. The legend is similar to Fig. 6.

B.3. Occultation of August 21, 2002

Elliot et al. (2003) derived an astrometric solution of the occultation by giving distance of closest approach to the centre of Pluto's shadow for Mauna Kea Observatory (597 ± 32 km) and Lick Observatory (600±32 km). They observed a positive occultation with three telescopes (two in Hawaii and one at Lick Observatory).

As there are at least two stations observing this occultation, there is a unique solution. According to the mid-time of the occultation in the two stations (see Table B.2), we derived the following offsets:

(g) 2014-07-23 (North solution)

(h) 2014-07-23 (South solution)

(i) 2014-07-24 (North solution)

(j) 2014-07-24 (South solution)

(k) 2015-06-29
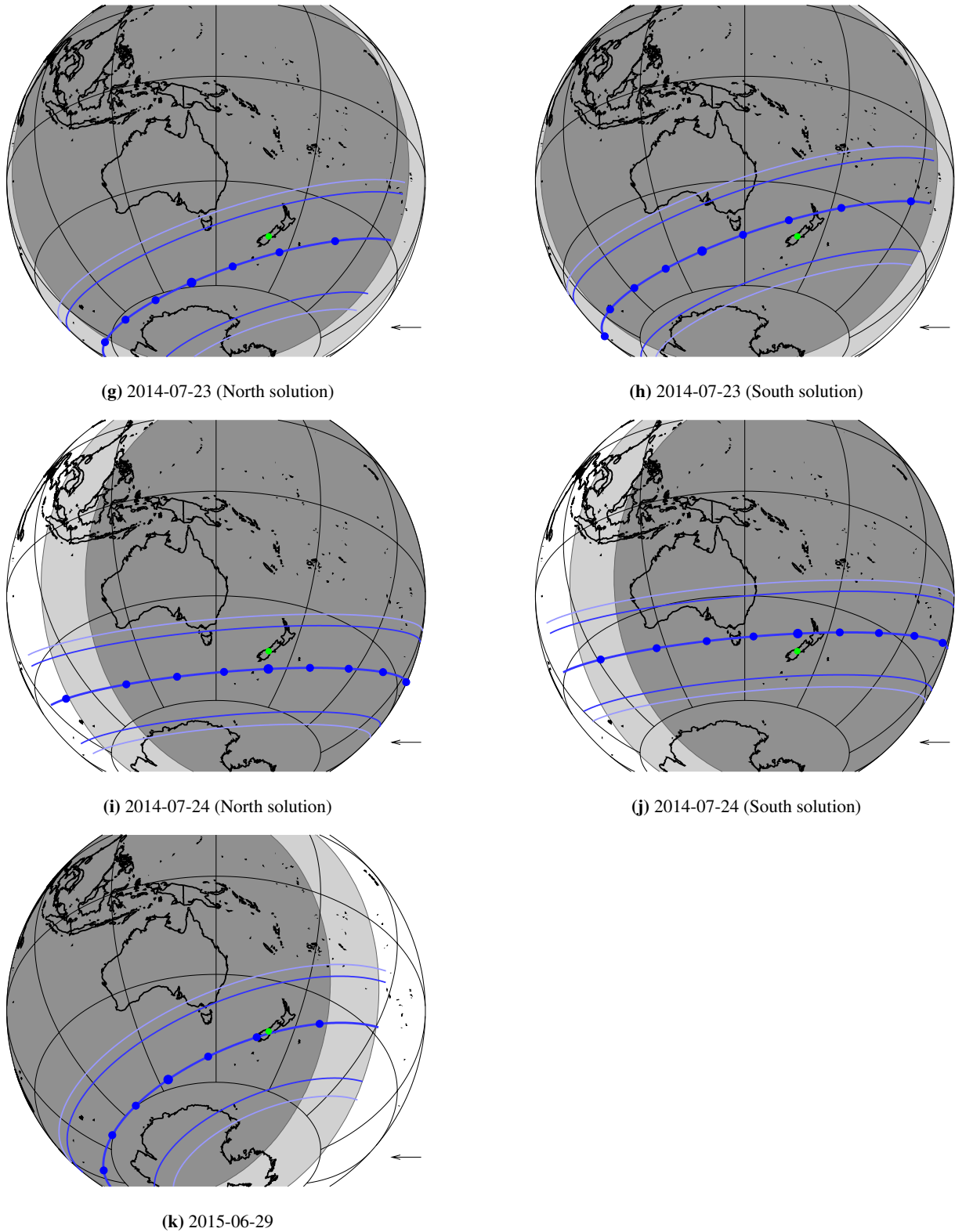
Fig. B.1. continued.

Finally, for this occultation, we used an average offset of $\Delta\alpha\cos\delta = +15.4 \pm 1.0$ mas and $\Delta\delta = -9.1 \pm 1.7$ mas.

B.4. Occultation of June 12, 2006

Young et al. (2008) presented the analysis of an occultation by Pluto on June 12, 2006. They published the half light time (ingress and egress) and the impact parameter (closest distance to the centre of the shadow) for five stations:

– REE = Reedy Creek Observatory, QLD, AUS (0.5 m aperture).
– AAT = Anglo-Australian Observatory, NSW, AUS (4 m).
– STO = Stockport Observatory, SA, AUS (0.5 m).
– HHT = Hawkesbury Heights, NSW, AUS (0.2 m).

Table B.1. Observatories and their associated mid-time and impact parameter of the occultation and the derived offset in timing, right ascension, and declination.

Observatory	Mid-time (UTC)	ρ (km)	Δt (s)	$\Delta\alpha\cos\delta$ (mas)	$\Delta\delta$ (mas)
Charters Towers	10:41:27.1 ± 1.23	985	130.0	20.6	−33.5
Toowoomba	10:40:50.5 ± 0.55	188	93.4	18.4	−33.6
Mt Tamborine	10:40:17.4 ± 0.95	168	60.3	−4.3	−33.9
Auckland	10:39:03.3 [1]	−687	−13.8	26.6	−33.9
Hobart	10:41:00.6 ± 1.95	−1153	103.5	19.5	−33.8
KAO	10:37:26.9 ± 0.15	868	−110.2	19.5	−33.0
Mt John	10:39:19.6 ± 0.78	−1281	2.5	19.9	−33.6

Notes. [1]Uncertainty of timing in Auckland is not provided in Millis et al. (1993).

Table B.2. Observatories and their associated mid-time and impact parameter of the occultation and the derived offset in timing, right ascension, and declination.

Observatory	Mid-time (UTC)	ρ (km)	Δt (s)	$\Delta\alpha\cos\delta$ (mas)	$\Delta\delta$ (mas)
CFHT 2.2m	6:50:33.9 ± 0.5	597	−598.1	16.0	−8.0
CFHT 0.6m	6:50:33.9 ± 1.8	597	−598.1	16.0	−8.2
Lick obs.	6:45:48.0 ± 2.8	600	−884.0	14.2	−11.0

Table B.3. Observatories and their associated mid-time and impact parameter of the occultation and the derived offset in timing, right ascension, and declination.

Observatory	Mid-time (UTC)	ρ (km)	Δt (s)	$\Delta\alpha\cos\delta$ (mas)	$\Delta\delta$ (mas)
REE	16:23:00.64 ± 2.61	836.6	−125.2	9.4	−0.5
AAT	16:23:19.67 ± 0.05	571.8	−106.1	9.6	−0.5
STO	16:23:59.62 ± 0.80	382.2	−66.2	9.7	−0.5
HHT	16:23:17.70 ± 2.12	302.5	−108.1	9.1	−0.4
CAR	16:22:30.82 ± 1.96	−857.6	−155.0	11.2	−0.4

– CAR = Carter Observatory, Wellington, NZ (0.6 m)

These parameters allow us to compute the mid-time of the occultation and to finally derive an offset for each station (see Table B.3).

Finally, for this occultation, we used an average offset of $\Delta\alpha\cos\delta = +9.8 \pm 0.8$ mas and $\Delta\delta = -0.4 \pm 0.1$ mas.

B.5. Occultation of March 18, 2007

Person et al. (2008) presented an analysis of an occultation by Pluto observed in several places in USA on March 18, 2007. From five stations, they derived the geometry of the event by providing the mid-time (UTC) of the event at 10:53:49 ± 00:01 (giving $\Delta t = -344.1$ s) and an impact parameter of 1319 ± 4 km for the Multiple Mirror Telescope Observatory (MMTO).

According to the geometry of the event, the south solution ($\rho = -1319$ km) has to be adopted, giving the offset related to JPL DE436/PLU055 ephemeris of $\Delta\alpha\cos\delta = 10.7 \pm 0.3$ mas and $\Delta\delta = 0.8 \pm 0.2$ mas.

B.6. Occultation of June 23, 2011

Gulbis et al. (2015) presented a grazing occultation by Pluto observed in IRTF (Mauna Kea Observatory) on June 23, 2011.

Table B.4. Derived offset in right ascension and declination associated to north and south solutions.

	North	South
$\Delta\alpha\cos\delta$ (mas)	16.1	5.3
$\Delta\delta$ (mas)	5.5	106.1

Table B.5. Derived offset in right ascension and declination associated to north and south solutions.

	North	South
$\Delta\alpha\cos\delta$ (mas)	30.3	22.9
$\Delta\delta$ (mas)	3.7	44.9

Table B.6. Derived offset in right ascension and declination associated to north and south solutions.

	North	South
$\Delta\alpha\cos\delta$ (mas)	3.4	11.3
$\Delta\delta$ (mas)	29.1	−14.6

They derived an impact parameter of 1138 ± 3 km and a mid-time (UTC) of the event at 11:23:03.07 (±0.10 s).

The single chord leads to two possible solutions providing the following offset related to JPL DE436/PLU055 ephemeris (see Table B.4).

According to Gulbis et al. (2015), the north solution has to be adopted. Finally, the offset is $\Delta\alpha\cos\delta = 16.1 \pm 0.1$ mas and $\Delta\delta = 5.5 \pm 0.1$ mas, assuming the estimated precision of the timing and the impact parameter.

B.7. Occultation of May 4, 2013

Olkin et al. (2015) presented the occultation by Pluto on May 4, 2013 observed in South America. They derived the mid-time (UTC) of the event at 08:23:21.60 ± 0.05 s (giving $\Delta t = 99.8$ s) and an impact parameter of 370 ± 5 km for the LCOGT at Cerro Tololo. From these circumstances, we derived an offset related to JPL DE436/PLU055 ephemeris of $\Delta\alpha\cos\delta = 18.7 \pm 0.1$ mas and $\Delta\delta = 8.4 \pm 0.2$ mas.

B.8. Occultation of July 23, 2014

Pasachoff et al. (2016) published the observation of two single-chord occultations at Mont John (New Zealand) on June 2014. They provided the timing and impact parameter for the two occultations.

The fitted impact parameter for July 23 is $\rho = 480 \pm 120$ km, providing two possible solutions and the mid-time (UTC) of the occultation 14:24:31 ± 4 s is derived from the ingress and egress times at 50% and corresponds to $\Delta t = -88.1$ s.

Each solution provides the following offset related to JPL DE436/PLU055 ephemeris (see Table B.5).

According to the precisions of the mid-time and of the impact parameter, the estimated precision of the offset is 4.0 mas for $\Delta\alpha\cos\delta$ and 5.2 mas for $\Delta\delta$.

B.9. Occultation of July 24, 2014

Pasachoff et al. (2016) also provided circumstances of the occultation on July 24, 2014 at Mont John Observatory.

The fitted impact parameter is $\rho = 510 \pm 140$ km providing two possible solutions and the mid-time (UTC) of the occultation $11:42:29 \pm 8$ s is derived from the ingress and egress times at 50% and corresponds to $\Delta t = 9.1$ s.

Each solution provides the following offset related to JPL DE436/PLU055 ephemeris (see Table B.6).

According to the precisions of the mid-time and impact parameter, the estimated precision of the offset is 7.7 mas for $\Delta\alpha \cos\delta$ and 6.1 mas for $\Delta\delta$.

B.10. Occultation of June 29, 2015

Pasachoff et al. (2017) presented the occultation by Pluto on June 29, 2015. They derived the mid-time (UTC) of the event at 16:52:50 (giving $\Delta t = -111.4$ s) and an impact parameter of -53.1 km for the Mont John Observatory in New Zealand.

From these circumstances, we derived an offset of $\Delta\alpha \cos\delta = 22.1$ mas and $\Delta\delta = 12.7$ mas related to JPL DE436/PLU055 ephemeris. The precision of the offset cannot be determined since the precision in mid-time and in the impact parameter are not indicated.

Table B.7. Besselian elements for occultations listed in the appendix derived with *Gaia* DR2 for the star's position and JPL DE436/PLU055 for Pluto's ephemeris.

T_0	x_0	y_0	x'	y'	H	α_s	δ_s
1988-06-09 10:39:17.1	0.006535856	−0.390599080	−242.990271254	−4.176391160	−47.003163462	223.041508925	0.750884462
2002-07-20 01:43:39.8	−0.015137748	0.078729716	−221.595155776	−42.613814665	45.303191676	255.075123563	−12.694996935
2002-08-21 07:00:32.0	0.091629552	−0.047418125	−41.470159949	−80.186411178	−27.314474978	254.705972362	−12.858853587
2006-06-12 16:25:05.8	0.008081468	−0.393907343	−320.357408358	−6.588025106	39.386450596	265.300310118	−15.692941450
2007-03-18 10:59:33.1	−0.283497691	0.985999061	92.267892934	26.509008184	−58.153737570	268.773723165	−16.476135950
2011-06-23 11:23:48.2	−0.043316318	0.403059932	−320.782100593	−34.487845936	50.562763031	276.481160400	−18.801937982
2013-05-04 08:21:41.8	0.013860759	−0.136954904	−137.646799082	−13.969616086	16.003277103	281.968884350	−19.690120815
2014-07-23 14:25:59.1	0.110372760	−0.614706119	−300.130385882	−53.903828467	−20.940785660	282.382245191	−20.373331983
2014-07-24 11:42:19.9	0.075661748	−0.419500350	−297.988040527	−53.754831391	−22.209299195	282.360471376	−20.376972931
2015-06-29 16:54:41.4	0.106938572	−0.628240925	−318.341422110	−54.232339089	−2.294494383	285.206150857	−20.694717628

Notes. T_0 is the UTC time of the closest approach, x_0, y_0 are the coordinates of the shadow axis in the fundamental plane at T_0 (in Earth's radius unit), x', y' are the rate of change in x and y at T_0 (in equatorial Earth's radius per day), H is the Greenwich Hour Angle of the star at T_0 (in degrees), and α_s, δ_s are the right ascension and declination of the star (in degrees).